

Localized dynamics following a quantum quench in a non-integrable system: An example on the sawtooth ladder

Rishabh Khare

Department of Physics and Astronomy, Purdue University, West Lafayette, IN 47907

Sayan Choudhury*

Department of Physics and Astronomy, University of Pittsburgh, Pittsburgh, PA 15260

(Dated: January 5, 2021)

Motivated by the recent discovery of ergodicity breaking in geometrically frustrated systems, we study the quench dynamics of interacting hardcore bosons on a sawtooth ladder. We identify a set of initial states for which this system exhibits characteristic signatures of localization like initial state memory retention and slow growth of entanglement entropy for a wide parameter regime. Remarkably, this localization persists even when the many-body spectrum is thermalizing. We argue that the localized dynamics originates from an interaction induced quantum interference. Our results show that the sawtooth ladder can be a fertile platform for realizing non-equilibrium quantum states of matter.

I. INTRODUCTION

The non-equilibrium dynamics of isolated quantum systems have received significant attention in recent years [1–25]. It is now well established that a large class of quantum many-body models are non-integrable, and any “typical” initial state would eventually thermalize in these systems. This thermalization is generally understood through the framework of the Eigenstate Thermalization Hypothesis (ETH) [26–32]. Important exceptions to the strong version of the ETH include Many-body localization (MBL) [33–44], Bethe-ansatz integrable systems [45–48], and quantum many-body scars [49–56]. Such non-ergodic states of matter provide a route towards preserving quantum coherence in many-body systems. Consequently, ETH violating quantum systems have served as a versatile platform for creating exotic non-equilibrium states of matter like discrete time crystals [57–62] and Floquet topological phases [63, 64].

Recently, some researchers have proposed a different route for realizing non-ergodic phases of matter: interacting flat band models without disorder [65–67]. These systems host localized single-particle eigenstates and their ground state is typically localized below a critical density [68]. Remarkably, in a recent study, Kuno *et al.* have demonstrated that the flat band structure can induce localized dynamics, both in the presence and absence of interactions [65]. An important question naturally rises in this context: does this localization persist away from the flat band limit, when the single-particle eigenstates are no longer localized?

We address this issue by studying the quench dynamics of hardcore bosons loaded in the sawtooth ladder. We demonstrate that for certain initial states,

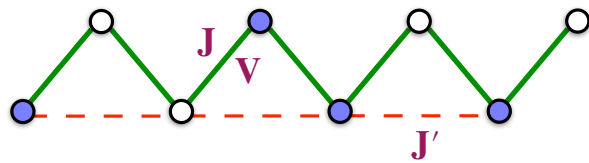


FIG. 1. Schematic representation of hardcore bosons on the sawtooth ladder. The nearest neighbor tunneling amplitude is J and the next-nearest neighbor tunneling amplitude at odd sites is J' . Furthermore, bosons on neighboring sites also experience an interaction V . This model hosts localized single-particle eigenstates, when $J = \sqrt{2}J'$.

this system can exhibit localized dynamics, both when the single band dispersion is flat and non-flat. Interestingly, this localization can be observed, even when the many-body spectrum is thermalizing. We trace the origin of this non-ergodicity to a destructive many-body interference. Our work establishes that the sawtooth ladder provides a promising avenue for creating non-equilibrium quantum matter.

This paper is organized as follows. In section II, we introduce our model and discuss its non-interacting limit. In section III, we study the quench dynamics of hardcore bosons on the sawtooth lattice at half-filling in the presence of nearest neighbor repulsive interactions. Employing both exact diagonalization as well as analytical calculations, we identify the conditions under which the system exhibits localized dynamics. Furthermore, we compute the eigenvalue spectrum, and demonstrate that localization can be observed even in a parameter regime where the system is ergodic. In section IV, we explore information propagation in the system by studying the growth of the half-chain entanglement entropy. We find that in the localized regime, the growth of the entanglement entropy is slow. We conclude with a summary of

* sayan.choudhury@pitt.edu

our results, a brief discussion of potential experimental realizations, and an outlook in section V.

II. MODEL

As illustrated in Fig. 1, we study the out-of-equilibrium dynamics of hardcore bosons on a sawtooth ladder. The Hamiltonian for this system is

$$H = \sum_{i=1}^{L/2} J(c_{A,i}^\dagger c_{B,i} + c_{B,i}^\dagger c_{A,i+1}) + J' c_{i,A}^\dagger c_{i+1,A} + \frac{V}{2} (n_{i,A} n_{i,B} + n_{i,B} n_{i+1,A}) + h.c., \quad (1)$$

where J is the nearest neighbor tunneling element, J' is the next-nearest tunneling element between odd sites, and V is the interaction between bosons on neighboring sites. This model can be solved exactly in the non-interacting limit, ($V \rightarrow 0$), where the open (periodic) spin chain hosts $L/2 - 1$ ($L/2$) compact localized (CL) eigenstates of the form:

$$|\psi\rangle_{\text{CL}} = \frac{1}{2} \left(c_{A,i-1}^\dagger - \sqrt{2} c_{B,i}^\dagger + c_{A,i}^\dagger \right) |0\rangle, \quad (2)$$

when, $J = \sqrt{2}J'$. These localized eigenstates lead to the formation of a flat band in the case of periodic boundary conditions.

The equilibrium properties of this model have been studied extensively [69–74]; its ground state is localized below a critical density of $1/4$ [75]. Furthermore, when the hardcore constraint is removed, this system can exhibit supersolidity [75] as well as topological order [76]. In this paper, we explore a less studied aspect of this model - its out-of-equilibrium dynamics. We employ open boundary conditions for these calculations; this choice is motivated by experimental considerations. Our results demonstrate that frustrated systems can exhibit rich dynamical behavior.

We solve this model using exact diagonalization. The total number of particles is a conserved quantity, and we fix it to be $L/2$. Thus, the Hilbert space dimension is reduced to $\mathbb{D} = \binom{L}{L/2}$. Furthermore, in this half-filling sector, the system has a particle-hole symmetry. We will account for this symmetry when we compute the level statistics in the next section.

III. QUENCH DYNAMICS AND EIGENVALUE STATISTICS

A. Quench Dynamics

Quantum quenches provide a very powerful tool to study non-equilibrium dynamics. A quench protocol typically involves preparing the system in the ground

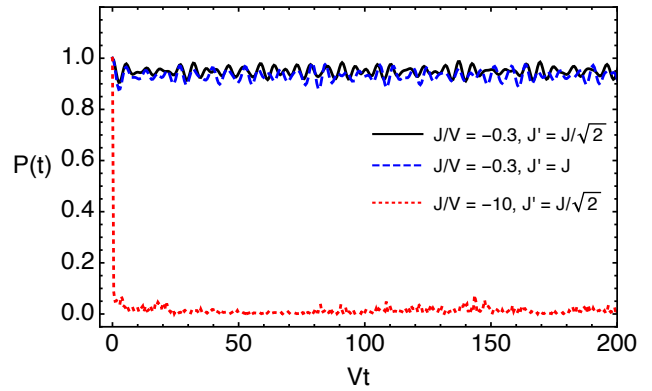


FIG. 2. The return probability, $P(T)$ (defined in Eq. 3) for the 12-site ladder, when the system is initially prepared in the “domain wall” state defined in Eq. (4). The memory of the initial state is retained for long time when $J/V \sim -0.3$, regardless of whether the single-particle eigenstates are localized or delocalized. On the other hand, the memory of the initial state is lost very fast when $|J/V| \gg 1$, even when the single-particle eigenstates are localized.

state of some initial Hamiltonian H_i and then studying its time evolution after a sudden change of parameters to some final Hamiltonian H_f [77]. Quantum quenches have been used to study many-body localization [37, 38], the dynamics of thermalization [78, 79], the Kibble-Zurek mechanism [80, 81], and even topological properties of a system like the linking number and Chern number [82–84]. In this section, we employ quench dynamics to study localization.

A salient characteristic that distinguishes localized systems from thermalizing systems is that localized systems can retain the memory of its initial state for very long times, while thermalizing systems lose this memory exponentially fast. This feature has been widely used to study localization in current experiments. We characterize the initial state memory retention in our model by computing the return (or survival) probability $P(t)$:

$$P(t) = |\langle \psi(t=0) | \exp(-iHt) | \psi(t=0) \rangle|^2, \quad (3)$$

where $|\psi(t=0)\rangle$ is the initial state of the system. This return probability is a type of Loschmidt echo that is used to probe non-equilibrium phenomena like dynamical quantum phase transitions [85–87] and many-body localization [88]. We assume that $|\psi(t=0)\rangle$ is an unentangled Fock state, in accordance with current experiments [37, 38]. Localization is indicated by a large value of $P(t)$ at long times [65].

We study the time evolution of the system, when it is initially prepared in the so called “domain wall” (DW) state:

$$|\psi(t=0)\rangle = |\psi_{\text{DW}}\rangle = |\dots \bullet \bullet \bullet \bullet \bullet \bullet \circ \circ \circ \circ \circ \circ \dots\rangle, \quad (4)$$

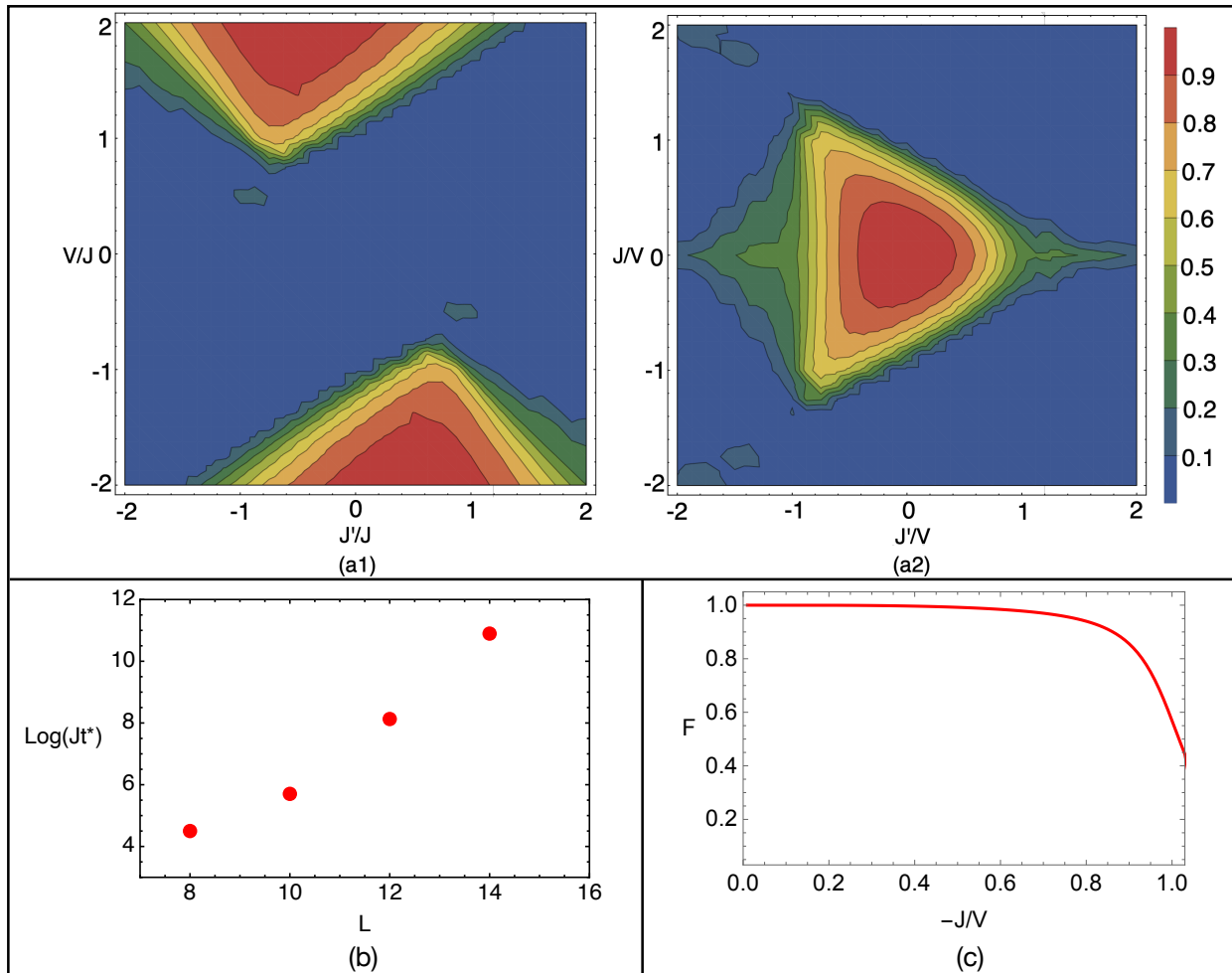


FIG. 3. (a1)-(a2) Contour plots of the average return probability, $P(t)$, for the 12-site ladder. For (a1), we show the average of $P(t)$ from $t = 0$ to $t = 1000/J$ as a function of V and J' . In (a2), we show the average of $P(t)$ from $t = 0$ to $t = 1000/V$ as a function of J and J' . It is clear from these plots that our model exhibits localized dynamics for a wide parameter regime. (b) Dependence of the localization lifetime, t^* on the system size, L , when $J'/V = -0.4$ and $J/V = -0.68$. We have defined t^* as the time, when $P(t)$ drops below 0.05. The lifetime appears to increase exponentially with the system size. (c) The overlap of the numerically obtained eigenstate $|\psi_{\text{loc}}\rangle$ with the analytic eigenstate $|\phi_{\text{loc}}\rangle$ for the 10-site ladder, when $J/V = J'/V$. This overlap, F (as defined in Eq. 7) is large (≥ 0.9) for a wide parameter regime, indicating that the state is localized.

where the first $L/2$ sites are occupied and the other half is empty. The DW state is an eigenstate of the Hamiltonian in the Ising limit ($\frac{J}{V} \rightarrow 0, \frac{J'}{V} \rightarrow 0$). Thus, the protocol described here is equivalent to a quantum quench, where the initial Hamiltonian is $H_0 = V(n_{i,A}n_{i,B} + n_{i,B}n_{i+1,A})$ and the final Hamiltonian is H . We note that this quench has been extensively studied in the integrable $J' \rightarrow 0$ limit [89–93].

As shown in Fig. 2, the return probability, $P(t)$ initially exhibits a transient decay. This behavior can be understood using perturbation theory:

$$\begin{aligned} P(t) &= 1 - \omega_{\text{ini}}^2 t^2 \\ &= 1 - (\langle \psi_{\text{DW}} | H^2 | \psi_{\text{DW}} \rangle - \langle \psi_{\text{DW}} | H | \psi_{\text{DW}} \rangle^2) t^2. \end{aligned} \quad (5)$$

The quadratic decay is expected to persist up to a

time $t \ll \frac{1}{\omega_{\text{ini}}}$. Following this transient regime, $P(t)$ can decay exponentially (for chaotic systems), or very slowly (for localized systems). For our model, we find that $P(t)$ decays rapidly, when $|J/V| \sim |J'/V| \gg 1$, while localized dynamics can be observed for smaller values of $|J/V| \sim |J'/V|$ (for instance when $J/V = -0.3$ and $J' \sim J$). We emphasize that this localization is qualitatively distinct from MBL in a number of aspects. Firstly unlike strongly disordered systems, bosons loaded in the sawtooth ladder exhibit initial state memory retention, both when the single-particle eigenstates are localized and delocalized. Furthermore, in this system, $P(t)$ fluctuates around an equilibrium value after the initial decay. On the other hand, $P(t)$ oscillates and then decays as a power law (before saturating) in many-body localized systems [88].

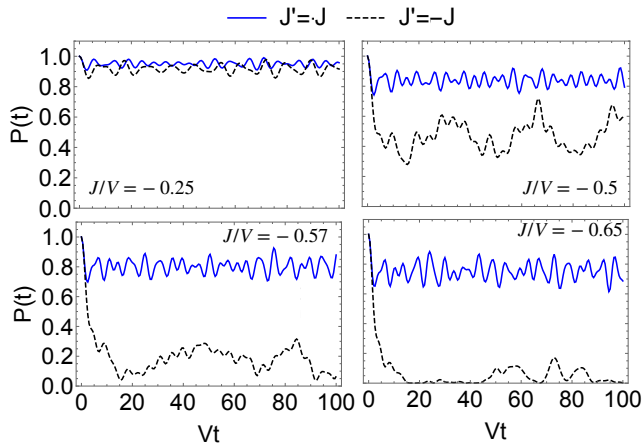


FIG. 4. The return probability for the 12-site ladder, when $J'/V = -0.25, -0.5, -0.57$ and -0.65 . The solid blue line (dashed black line) shows $P(t)$ when J' equals $J(-J)$. The localization is enhanced when J'/V is negative, thus complementing the results from Fig. 3.

We carefully study the long time behavior of $P(t)$ and find a considerable enhancement in both the parameter regime for observing localization (Fig. 3(a2)) and the localization strength (Fig. 4), when J'/V is negative. As explained in the next sub-section, this phenomenon originates from a many-body destructive interference. Furthermore, we examine the localization lifetime by identifying the time t^* , when $P(t)$ drops below 0.05. Figure 3(b) shows that the localization lifetime appears to increase exponentially with the size of the system. This indicates that the localization will persist in the limit of infinite system size.

B. Effective Analytical Model

In the last sub-section, we have demonstrated that there is a wide parameter regime for which our model exhibits localization. By carefully examining the eigenstates of the Hamiltonian, H defined in Eq. (1), we find that this localized dynamics arises due to the existence of localized eigenstates. We now proceed to derive an approximate analytic form for the localized eigenstate, $|\psi_{\text{loc}}\rangle$ that has a large overlap with the DW state, $|\psi_{\text{DW}}\rangle$.

It is possible to obtain an analytical form for the localized eigenstate near the Ising limit i.e. when $|J/V| \simeq |J'/V| \ll 1$. In particular, when $L = 4m + 2$, we use second order perturbation theory to obtain the following expression for the localized eigenstate, $|\psi_{\text{loc}}\rangle =$

$|\phi_{\text{loc}}\rangle + \dots$, where:

$$|\phi_{\text{loc}}\rangle = \frac{1}{\sqrt{2}} \left(|\phi_1\rangle + \left(\frac{J}{V} + \frac{J'J}{V^2}\right)|\phi_2\rangle + \left(\frac{J'}{V} + \frac{J^2}{V^2}\right)|\phi_3\rangle \right), \quad (6)$$

and

$$\begin{aligned} |\phi_1\rangle &= |\dots \bullet \bullet \bullet \bullet \circ \circ \circ \circ \dots\rangle + |\dots \circ \circ \circ \circ \bullet \bullet \bullet \bullet \dots\rangle \\ |\phi_2\rangle &= |\dots \bullet \bullet \bullet \circ \bullet \circ \circ \circ \dots\rangle + |\dots \circ \circ \circ \bullet \circ \bullet \bullet \bullet \dots\rangle \\ |\phi_3\rangle &= |\dots \bullet \bullet \bullet \circ \circ \bullet \circ \circ \dots\rangle + |\dots \circ \circ \circ \bullet \circ \bullet \bullet \bullet \dots\rangle \end{aligned}$$

It is clear from this expression that when J'/V is negative, the amplitudes of $|\phi_1\rangle$, and $|\phi_2\rangle$ are suppressed, and this in turn can suppress states that appear in higher order in perturbation theory. This implies that in this model, a destructive many-body interference causes localization. In order to determine the validity of our analytic approximation, we compute the overlap of the analytic eigenstate, $|\phi_{\text{loc}}\rangle$ with the numerically obtained eigenstate, $|\psi_{\text{loc}}\rangle$:

$$F = |\langle \phi_{\text{loc}} | \psi_{\text{loc}} \rangle|. \quad (7)$$

Figure 3(c) shows that our analytical results agree well with the numerically obtained eigenstate, $|\psi_{\text{loc}}\rangle$ for a large parameter regime. In particular, we note that $F \geq 0.9$, even when $J'/V \sim J/V \sim -0.8$, and the system is well outside the Ising limit. This result also agrees with the phase diagram in Fig. 3(a2).

Furthermore, from the argument outlined above, we can conclude that localization can be observed for any initial state for which the domain walls are separated by distance, $d \gg a$, where a is the distance between neighboring A sites. Thus, the number of localized states in our model are expected to grow with the size of the system. Moreover, in the quench protocol that we have discussed, the return probability would be maximum for the domain wall initial state.

C. Level Statistics

A possible explanation for the observed localization behavior is that our model is integrable. To verify this explanation, we examine the spectral statistics of our model. This diagnostic is frequently used to distinguish integrable models from non-integrable ones [94, 95]. Integrable systems are characterized by Poisson level statistics, while non-integrable systems exhibit pronounced level repulsion and the distribution of energy level spacings is described by the Wigner-Dyson distribution [96, 97].

We analyze the level statistics of our model following the standard procedure outlined in the literature [98, 99]. We first diagonalize the Hamiltonian, only retaining the eigenstates in one symmetry sector.

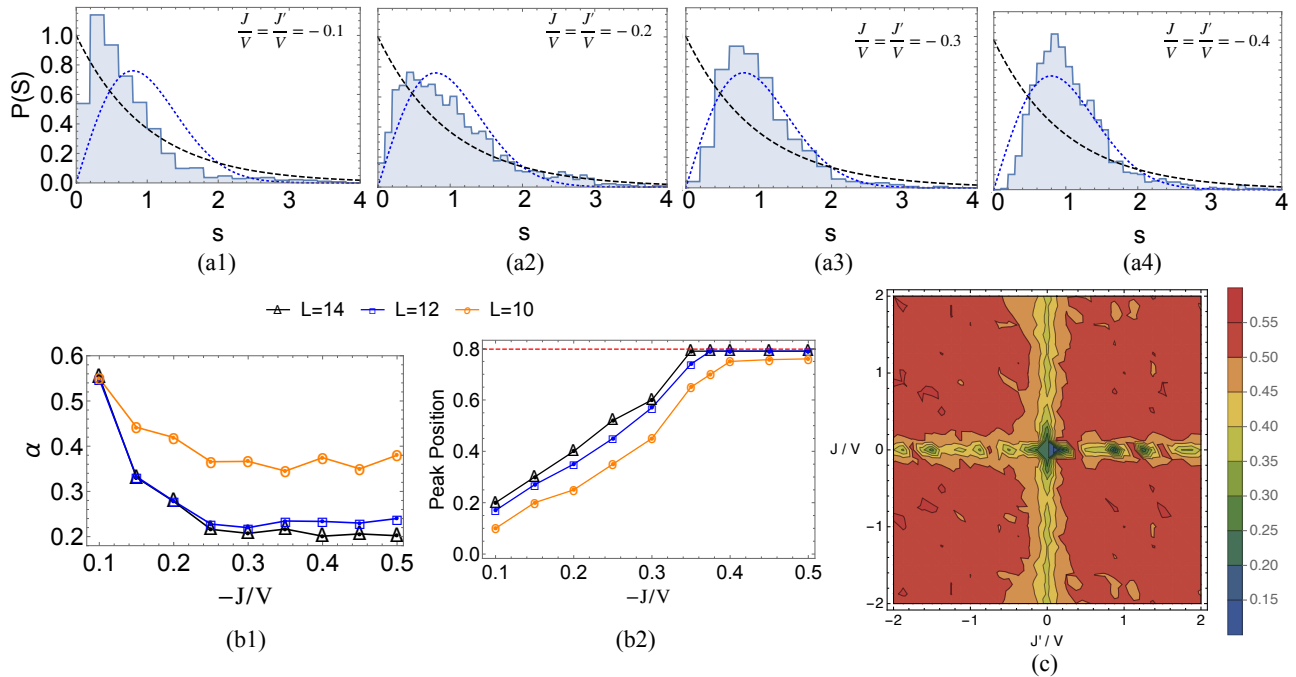


FIG. 5. (a1)-(a4): Level spacing distribution for the 14-site sawtooth ladder. The black (dashed) and blue (dotted) curves show the Poisson and Wigner-Dyson distribution respectively. The model exhibits a transition from integrability to chaos with increasing $|J|$ and $|J'|$. (b1)-(b2): The level spacing indicator α (defined in Eq. 8) and the peak position of $P(s)$ for different values of $J/V = J'/V$ and three system sizes. The red (dashed) line in (b2) indicates the peak of the Wigner-Dyson distribution, $P_{\text{WD}}(s)$. (c) Contour plot of $\langle r \rangle$ (defined below Eq. 10) for the 12-site ladder. It is evident that the model is chaotic ($\langle r \rangle \approx 0.53$) for a large region of parameter space.

This is done by accounting for the two symmetries of our model at half-filling: total particle number conservation and particle-hole symmetry. In particular, we retain only the states in the $\mathcal{P} = 1$ sector, where \mathcal{P} is the eigenvector of the particle-hole transformation operator, $\prod_i (c_{A,i}^\dagger + c_{A,i})(c_{B,i}^\dagger + c_{B,i})$; the number of such states is $\overline{\mathbb{D}} = \mathbb{D}/2 = \frac{1}{2} \binom{L}{L/2}$. We then proceed to compute the distribution P of neighboring energy level spacings s . The distribution is Poisson-like in the Ising limit; as $|J/V|, |J'/V|$ increases, the peak of $P(s)$ shifts to the right and its tail becomes Gaussian. Our results are shown in top panel of Fig. 5

In order to probe the transition from integrability to chaos, we compute the level spacing indicator, α [99]:

$$\alpha = \frac{\sum_i |P(s_i) - P_{\text{WD}}(s_i)|}{\sum_i P_{\text{WD}}(s_i)}, \quad (8)$$

where $P_{\text{WD}}(s) = (\pi s/2) \exp(-\pi s^2/4)$ is the Wigner-Dyson distribution. In the integrable regime, $P(s)$ is close to the Poisson distribution ($\exp(-s)$), and $\alpha \rightarrow 0.615$, while the chaotic regime is characterized by $\alpha \rightarrow 0$. We find that α is close to 0.6 near the Ising limit ($J/V \sim J'/V \sim -0.1$); it decreases for larger values of $|J/V|, |J'/V|$ and eventually saturates to a value that decreases with increasing system size (see Fig. 5(b1)). We note however that α does not reach

zero for the small ladders considered here.

Furthermore, we compute the peak position of $P(s)$ and demonstrate that it approaches the peak of the Wigner Dyson distribution with increasing $|J/V|$ and $|J'/V|$. Our results are shown in Fig. 5(b2). This analysis is equivalent to fitting $P(s)$ to the Brody distribution [99, 100]:

$$P_\beta(s) = (\beta + 1) b s^\beta \exp(-b s^{\beta+1}), \quad b = \left[\Gamma\left(\frac{\beta + 2}{\beta + 1}\right) \right]^{\beta+1}, \quad (9)$$

and examining how β changes with increasing $|J/V|$ and $|J'/V|$. Both of these aforementioned metrics indicate that the model is chaotic for a wide parameter regime, and the transition to chaos occurs at decreasing values of $|J/V|, |J'/V|$ with increasing system size. Much larger system sizes are required to determine the critical parameter value at which this transition occurs.

A complimentary approach to analyze the level statistics was introduced by Oganessian and Huse [101]. They computed the ratios of the neighboring energy gaps:

$$r_n = \frac{\min(s_n, s_{n+1})}{\max(s_n, s_{n+1})}, \quad (10)$$

and then averaged these ratios over all eigenstates to obtain $\langle r \rangle$. The Wigner Dyson distribution corresponds

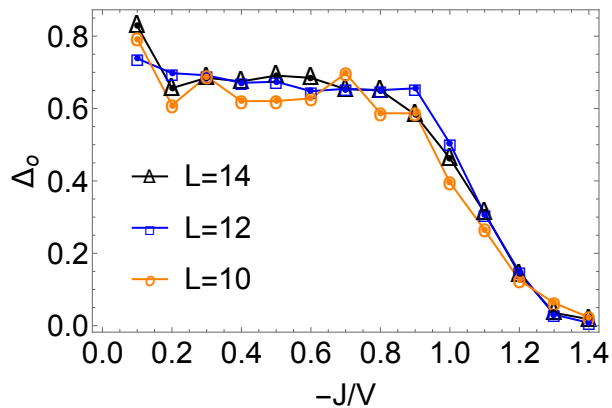


FIG. 6. The relative difference between the infinite time average and microcanonical average Δ_0 (defined in Eq. 14), when $J/V = J'/V$ and $L = 10, 12$, and 14 . The initial state is the domain wall state and the microcanonical window is taken to be $[E_{\text{ini}} - \delta E, E_{\text{ini}} + \delta E]$, where $\delta E = 1.5V$. There is a large parameter regime where thermalization does not occur, even though the model is chaotic.

to $\langle r \rangle \approx 0.53$, whereas the Poisson distribution is characterized by $\langle r \rangle \approx 0.39$ [102]. Figure 5(c) shows $\langle r \rangle$ for a 12-site ladder. We find that there is a wide parameter regime where the system exhibits localization, even though the spectrum is thermalizing ($\langle r \rangle \approx 0.53$). The presence of these localized states may be considered as an example of weak ergodicity breaking. To further substantiate this finding, we proceed to examine the nature of the post-quench equilibrium state of the system.

D. Equilibration and Thermalization

To determine whether a system has thermalized, we consider the time evolution of an observable, O :

$$\begin{aligned} \langle O(t) \rangle &= \langle \psi(t=0) | \exp(iHt) O \exp(iHt) | \psi(t=0) \rangle \\ &= \sum_{\mu, \nu} O_{\mu\nu} C^{\mu*} C^{\nu} \exp(-i(E_{\nu} - E_{\mu})t), \end{aligned} \quad (11)$$

where $C^{\nu} = \langle \psi_{\nu} | \psi(t=0) \rangle$, $\psi_{\nu}(E_{\nu})$ are the eigenvectors (eigenvalues) of H and $O_{\mu\nu} = \langle \psi_{\mu} | O | \psi_{\nu} \rangle$. The system equilibrates if $\langle O(t) \rangle$ remains close to the infinite time average, O_{DE} at most times, where:

$$O_{\text{DE}} = \sum_{\nu=1}^{\mathbb{D}} O_{\nu\nu} |C^{\nu}|^2. \quad (12)$$

The infinite time average is also referred to as the diagonal ensemble (DE) average, since it only depends on the diagonal elements of O . Equilibration would occur as long as there are not too many degeneracies in the spectrum. As shown in figures 2 and 4, $P(t)$ fluctuates around an equilibrium value after a short transient.

Thermalization occurs if O_{DE} coincides with the thermal average, O_{ME} defined as [103, 104]:

$$O_{\text{ME}} = \frac{1}{\mathcal{N}_E} \sum_{|E_{\text{ini}} - E_{\nu}| < \delta E} O_{\nu\nu}, \quad (13)$$

where E_{ini} is the energy of the initial state, \mathcal{N}_E is the number of eigenstates in the window δE around E_{ini} . We have chosen the observable $O = \frac{1}{L} \sum_i (\sigma_i^x \sigma_{i+1}^x + \sigma_i^y \sigma_{i+1}^y)$ and $\Delta E = 1.5V$. We have verified that our results do not depend on the precise value of ΔE , as long as there are a reasonably large number of states ($\sim 10^2$) in this window. We compute the relative difference between O_{ME} and O_{DE} :

$$\Delta_0 = \left| \frac{O_{\text{DE}} - O_{\text{ME}}}{O_{\text{DE}} + O_{\text{ME}}} \right|. \quad (14)$$

Figure 6 shows that the two averages do not coincide for a large parameter regime, indicating that this system does not thermalize. These findings reinforce our conclusion of weak ergodicity breaking.

IV. ENTANGLEMENT ENTROPY

Slow information propagation is another crucial aspect of localized many-body systems [34, 105]. Information propagation can be characterized by the growth of the half-chain entanglement entropy, and it serves as an important diagnostic that distinguishes MBL from Anderson localization [106, 107]. In this section, we study the growth of the entanglement entropy to examine whether our model exhibits characteristic features that distinguish it from both Anderson and many-body localization.

The half-chain entanglement entropy S_{ent} is defined as

$$S_{\text{ent}} = -\text{Tr}(\rho_L \log \rho_L), \quad (15)$$

where ρ_L is the reduced density matrix of the left half of the chain. It is obtained by tracing over the degrees of freedom of the right half of the chain:

$$\rho_L = \text{Tr}_R(|\psi\rangle\langle\psi|). \quad (16)$$

In order to compare the dynamical properties of our model to MBL, we examine the growth of the entanglement entropy, $S_{\text{ent}}(t)$ for three different parameters - one corresponding to delocalized and the others corresponding to localized dynamics. Our results are shown in Fig. 7.

We find that the entanglement entropy grows very fast up to times, $t \sim 1/|J|$, irrespective of whether the dynamics is localized or delocalized. Following this transient regime, the growth of the entanglement entropy

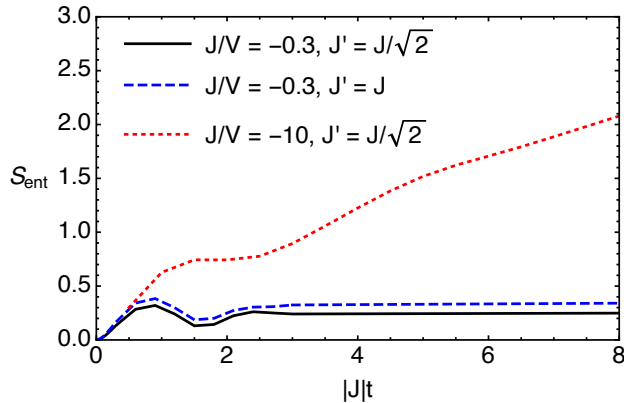


FIG. 7. The growth of the half-chain entanglement entropy, S_{ent} (defined in Eq. 15) for the 12-site ladder, following the quantum quench protocol discussed in section III. The entanglement entropy grows very slowly when the system exhibits localized dynamics. This is in sharp contrast to the fast growth of entanglement entropy observed when the dynamics is delocalized.

qualitatively mirrors the decay of the return probability; S_{ent} saturates (grows rapidly) in the localized (delocalized) regime. We note that unlike our model, S_{ent} grows logarithmically (remains 0) in many-body (Anderson) localized systems [105–107].

V. CONCLUSION AND OUTLOOK

In this paper, we have studied the dynamics of hardcore bosons loaded in the sawtooth ladder at half-filling. We have demonstrated that this system exhibits localized dynamics after a quantum quench for certain initial states. We show that this localization arises due to a many-body destructive interference and it can be observed for a wide parameter regime. Intriguingly, the localization persists even when this model is non-integrable, indicating that the ETH is weakly violated for this system. This finding is further validated by the absence of a post-quench thermalized state. Finally, we have examined the time evolution of the half chain entanglement entropy, and found that the entropy saturates after a transient regime. This behavior is qualitatively different from many-body localized systems, where the entropy grows logarithmically. Our results clearly establish that the sawtooth ladder geometry is a versatile platform for creating non-ergodic states of matter.

Our predictions can be verified in a variety of quantum emulator platforms. Zhang and Jo have proposed a realistic experimental scheme to realize the sawtooth ladder geometry in cold atomic gases [108]; the nearest neighbor interaction, V can be engineered using Rydberg atoms [109–112], ultracold molecules [113–116], or atoms loaded in a photonic crystal

waveguide [117]. Alternatively, this model can be realized in superconducting qubit processors [118–120] or by performing hybrid digital-analog simulations with trapped ions [121, 122]. Interestingly, Choi *et al.* have studied a quench starting from the two dimensional analog of the DW state in a cold atom experiment [38].

Our paper also suggests the possibility of using the sawtooth ladder for realizing non-equilibrium phases of matter like discrete time crystals. Furthermore, the localized states that we have found may also be used for making quantum memories [123], as well as for performing thermodynamic tasks [124]. We plan to explore these possibilities in the future.

ACKNOWLEDGEMENTS

We thank Qi Zhou, Bing Zhu, Johannes Majer, Xiaopeng Li, and Sayandip Dhara for fruitful discussions. This work is supported by the AFOSR Grant No. FA9550-16-1-0006, and the MURI-ARO Grant No. W911NF17-1-0323 (SC) and the Purdue Research Foundation (RK).

Update: When this manuscript was being finalized, we noted a recent preprint that outlines a scheme for realizing flat band many-body localization irrespective of the density or dimensionality of the system, as long as all single bands are flat [125]. The results from that study do not apply to the sawtooth ladder, where only one flat band is possible. In another recent preprint, McClarty *et al.* have demonstrated that the sawtooth ladder can exhibit weak ergodicity breaking due to the presence of quantum many-body scars [126].

Appendix A: Long Time Dynamics for other initial states

In the main text, we have explicitly demonstrated that hardcore bosons loaded in a sawtooth lattice can exhibit localized dynamics, when the system is initially prepared in the domain wall initial state defined in Eq. (4). As explained in sec. III B, this localization arises due to a many-body destructive interference. Our analysis naturally suggests that this system would exhibit localized dynamics, when it is initially prepared in a state in which the domain walls are separated by a distance, $d \gg a$, where the lattice parameter a is the distance between neighboring A sites.

We have tested this hypothesis by carefully studying the time evolution of this system, when it is initially prepared in an unentangled Fock state for system sizes, $L = 8, 10, 12$ and 14. For these small system sizes, we have found that in addition to the domain wall initial

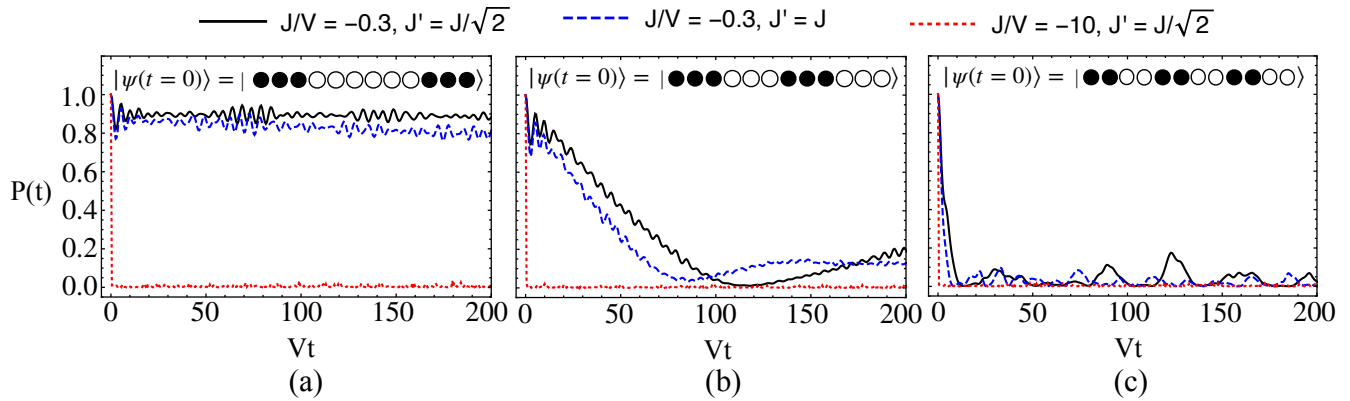


FIG. 8. (a)-(c): Return probability, $P(t)$ for the 12– site ladder, when the domain walls are separated by a distance $d/a = 6$, $d/a = 3$, and $d/a = 2$ respectively, where the lattice parameter a is defined in the main text. The many-body spectrum is thermalizing in all of these cases. The system exhibits localized dynamics only for case (a), when the domain walls are separated by a distance of $L/2$ for the parameters studied here. $P(t)$ decreases more and more rapidly as the number of domain walls increases.

state, localized dynamics can be observed for an initial state in which the domain walls are separated by a distance, $d/a = L/2$; the return probability decreases faster as the number of domain walls are increased.

Moreover, we observed that for most initial states, the return probability decreases very fast, since the model is chaotic in nature. Our results for the 12–site ladder are shown in Fig. 8.

-
- [1] D. A. Abanin, E. Altman, I. Bloch, and M. Serbyn, *Reviews of Modern Physics* **91**, 021001 (2019).
- [2] J. M. Deutsch, *Reports on Progress in Physics* **81**, 082001 (2018).
- [3] A. Dymarsky, N. Lashkari, and H. Liu, *Physical Review E* **97**, 012140 (2018).
- [4] S. Parameswaran and R. Vasseur, *Reports on Progress in Physics* **81**, 082501 (2018).
- [5] M. Rispoli, A. Lukin, R. Schittko, S. Kim, M. E. Tai, J. Léonard, and M. Greiner, *Nature* **573**, 385 (2019).
- [6] F. Borgonovi, F. M. Izrailev, and L. F. Santos, *Physical Review E* **99**, 010101 (2019).
- [7] C. Murthy and M. Srednicki, *Physical Review E* **100**, 012146 (2019).
- [8] Y. Tang, W. Kao, K.-Y. Li, S. Seo, K. Mallayya, M. Rigol, S. Gopalakrishnan, and B. L. Lev, *Physical Review X* **8**, 021030 (2018).
- [9] K. Mallayya, M. Rigol, and W. De Roeck, *Physical Review X* **9**, 021027 (2019).
- [10] T. B. Wahl, A. Pal, and S. H. Simon, *Nature Physics* **15**, 164 (2019).
- [11] Z. Lan, M. van Horssen, S. Powell, and J. P. Garrahan, *Physical Review Letters* **121**, 040603 (2018).
- [12] C. Chen, F. Burnell, and A. Chandran, *Physical Review Letters* **121**, 085701 (2018).
- [13] V. Khemani, A. Vishwanath, and D. A. Huse, *Physical Review X* **8**, 031057 (2018).
- [14] A. Nahum, S. Vijay, and J. Haah, *Physical Review X* **8**, 021014 (2018).
- [15] B. Skinner, J. Ruhman, and A. Nahum, *Physical Review X* **9**, 031009 (2019).
- [16] V. Khemani, D. A. Huse, and A. Nahum, *Physical Review B* **98**, 144304 (2018).
- [17] A. Nahum, J. Ruhman, and D. A. Huse, *Physical Review B* **98**, 035118 (2018).
- [18] S. Choudhury, E.-A. Kim, and Q. Zhou, arXiv:1807.05969 (2018).
- [19] S. Pai, M. Pretko, and R. M. Nandkishore, *Physical Review X* **9**, 021003 (2019).
- [20] K. A. Landsman, C. Figgatt, T. Schuster, N. M. Linke, B. Yoshida, N. Y. Yao, and C. Monroe, *Nature* **567**, 61 (2019).
- [21] A. Chenu, I. L. Egusquiza, J. Molina-Vilaplana, and A. del Campo, *Scientific Reports* **8**, 12634 (2018).
- [22] V. Alba and P. Calabrese, *Physical Review B* **100**, 115150 (2019).
- [23] Z. Li, S. Choudhury, and W. V. Liu, arXiv:2004.11269 (2020).
- [24] A. Keleş, E. Zhao, and W. V. Liu, *Physical Review A* **99**, 053620 (2019).
- [25] X.-L. Qi, E. J. Davis, A. Periwai, and M. Schleier-Smith, arXiv:1906.00524 [quant-ph] (2019).
- [26] M. Srednicki, *Physical Review E* **50**, 888 (1994).
- [27] J. M. Deutsch, *Physical Review A* **43**, 2046 (1991).
- [28] F. Borgonovi, F. M. Izrailev, L. F. Santos, and V. G. Zelevinsky, *Physics Reports* **626**, 1 (2016).
- [29] H. Kim, T. N. Ikeda, and D. A. Huse, *Physical Review E* **90**, 052105 (2014).
- [30] R. Steinigeweg, A. Khodja, H. Niemeyer, C. Gogolin, and J. Gemmer, *Physical Review Letters* **112**, 130403 (2014).
- [31] R. Steinigeweg, J. Herbrych, and P. Prelovšek, *Physical Review E* **87**, 012118 (2013).
- [32] M. Rigol, V. Dunjko, and M. Olshanii, *Nature* **452**, 854 (2008).
- [33] A. Pal and D. A. Huse, *Physical Review B* **82**, 174411

- (2010).
- [34] R. Nandkishore and D. A. Huse, *Annu. Rev. Condens. Matter Phys.* **6**, 15 (2015).
- [35] D. M. Basko, I. L. Aleiner, and B. L. Altshuler, *Annals of physics* **321**, 1126 (2006).
- [36] I. Aleiner, B. Altshuler, and G. Shlyapnikov, *Nature Physics* **6**, 900 (2010).
- [37] M. Schreiber, S. S. Hodgman, P. Bordia, H. P. Lüschen, M. H. Fischer, R. Vosk, E. Altman, U. Schneider, and I. Bloch, *Science* **349**, 842 (2015).
- [38] J.-Y. Choi, S. Hild, J. Zeiher, P. Schauß, A. Rubio-Abadal, T. Yefsah, V. Khemani, D. A. Huse, I. Bloch, and C. Gross, *Science* **352**, 1547 (2016).
- [39] M. Žnidarič, T. Prosen, and P. Prelovšek, *Physical Review B* **77**, 064426 (2008).
- [40] J. A. Kjäll, J. H. Bardarson, and F. Pollmann, *Physical Review Letters* **113**, 107204 (2014).
- [41] F. Alet and N. Laflorencie, *Comptes Rendus Physique* **19**, 498 (2018).
- [42] J. Smith, A. Lee, P. Richerme, B. Neyenhuis, P. W. Hess, P. Hauke, M. Heyl, D. A. Huse, and C. Monroe, *Nature Physics* **12**, 907 (2016).
- [43] D. A. Abanin and Z. Papić, *Annalen der Physik* **529**, 1700169 (2017).
- [44] J. Z. Imbrie, *Journal of Statistical Physics* **163**, 998 (2016).
- [45] C.-N. Yang and C. P. Yang, *Journal of Mathematical Physics* **10**, 1115 (1969).
- [46] M. Takahashi, *Thermodynamics of one-dimensional solvable models* (Cambridge University Press, 2005).
- [47] B. Pozsgay, *Journal of Statistical Mechanics: Theory and Experiment* **2011**, P01011 (2011).
- [48] V. B. Bulchandani, R. Vasseur, C. Karrasch, and J. E. Moore, *Physical Review Letters* **119**, 220604 (2017).
- [49] H. Bernien, S. Schwartz, A. Keesling, H. Levine, A. Omran, H. Pichler, S. Choi, A. S. Zibrov, M. Endres, M. Greiner, V. Vuletić, and M. D. Lukin, *Nature* **551**, 579 (2017).
- [50] C. J. Turner, A. A. Michailidis, D. A. Abanin, M. Serbyn, and Z. Papić, *Nature Physics* **14**, 745 (2018).
- [51] W. W. Ho, S. Choi, H. Pichler, and M. D. Lukin, *Physical Review Letters* **122**, 040603 (2019).
- [52] S. Choi, C. J. Turner, H. Pichler, W. W. Ho, A. A. Michailidis, Z. Papić, M. Serbyn, M. D. Lukin, and D. A. Abanin, *Physical Review Letters* **122**, 220603 (2019).
- [53] S. Moudgalya, N. Regnault, and B. A. Bernevig, *Physical Review B* **98**, 235156 (2018).
- [54] C.-J. Lin and O. I. Motrunich, *Physical Review Letters* **122**, 173401 (2019).
- [55] B. Mukherjee, S. Nandy, A. Sen, D. Sen, and K. Sengupta, *Physical Review B* **101**, 245107 (2020).
- [56] K. Lee, R. Melendrez, A. Pal, and H. J. Changlani, *Physical Review B* **101**, 241111(R) (2020).
- [57] V. Khemani, A. Lazarides, R. Moessner, and S. L. Sondhi, *Physical Review Letters* **116**, 250401 (2016).
- [58] C. W. von Keyserlingk, V. Khemani, and S. L. Sondhi, *Physical Review B* **94**, 085112 (2016).
- [59] J. Zhang, P. Hess, A. Kyprianidis, P. Becker, A. Lee, J. Smith, G. Pagano, I.-D. Potirniche, A. C. Potter, A. Vishwanath, N. Y. Yao, and C. Monroe, *Nature* **543**, 217 (2017).
- [60] S. Choi, J. Choi, R. Landig, G. Kucsko, H. Zhou, J. Isoya, F. Jelezko, S. Onoda, H. Sumiya, V. Khemani, C. von Keyserlingk, N. Y. Yao, E. Demler, and M. D. Lukin, *Nature* **543**, 221 (2017).
- [61] D. V. Else, B. Bauer, and C. Nayak, *Physical Review Letters* **117**, 090402 (2016).
- [62] N. Y. Yao, A. C. Potter, I.-D. Potirniche, and A. Vishwanath, *Physical Review Letters* **118**, 030401 (2017).
- [63] I.-D. Potirniche, A. C. Potter, M. Schleier-Smith, A. Vishwanath, and N. Y. Yao, *Physical Review Letters* **119**, 123601 (2017).
- [64] Y. Baum and G. Refael, *Physical Review Letters* **120**, 106402 (2018).
- [65] Y. Kuno, T. Orito, and I. Ichinose, *New Journal of Physics* **22**, 013032 (2020).
- [66] N. Roy, A. Ramachandran, and A. Sharma, arXiv:1912.09951 (2019).
- [67] S. Tilleke, M. Daumann, and T. Dahm, *Zeitschrift für Naturforschung A* **75**, 393 (2020).
- [68] R. Mondaini, G. G. Batrouni, and B. Grémaud, *Physical Review B* **98**, 155142 (2018).
- [69] O. Derzhko, J. Richter, A. Honecker, M. Maksymenko, and R. Moessner, *Physical Review B* **81**, 014421 (2010).
- [70] J. Richter, O. Derzhko, and A. Honecker, *International Journal of Modern Physics B* **22**, 4418 (2008).
- [71] V. R. Chandra, D. Sen, N. Ivanov, and J. Richter, *Physical Review B* **69**, 214406 (2004).
- [72] J. Richter, J. Schulenburg, A. Honecker, J. Schnack, and H.-J. Schmidt, *Journal of Physics: Condensed Matter* **16**, S779 (2004).
- [73] H.-J. Schmidt, J. Richter, and R. Moessner, *Journal of Physics A: Mathematical and General* **39**, 10673 (2006).
- [74] D. Sen, B. S. Shastri, R. Walstedt, and R. Cava, *Physical Review B* **53**, 6401 (1996).
- [75] S. D. Huber and E. Altman, *Physical Review B* **82**, 184502 (2010).
- [76] B. Grémaud and G. G. Batrouni, *Physical Review B* **95**, 165131 (2017).
- [77] A. Mitra, *Annual Review of Condensed Matter Physics* **9**, 245 (2018).
- [78] M. Rigol, *Physical Review A* **80**, 053607 (2009).
- [79] A. M. Kaufman, M. E. Tai, A. Lukin, M. Rispoli, R. Schittko, P. M. Preiss, and M. Greiner, *Science* **353**, 794 (2016).
- [80] D. Chen, M. White, C. Borries, and B. DeMarco, *Physical Review Letters* **106**, 235304 (2011).
- [81] L. W. Clark, L. Feng, and C. Chin, *Science* **354**, 606 (2016).
- [82] W. Sun, C.-R. Yi, B.-Z. Wang, W.-W. Zhang, B. C. Sanders, X.-T. Xu, Z.-Y. Wang, J. Schmiedmayer, Y. Deng, X.-J. Liu, S. Chen, and J.-W. Pan, *Physical Review Letters* **121**, 250403 (2018).
- [83] C. Wang, P. Zhang, X. Chen, J. Yu, and H. Zhai, *Physical Review Letters* **118**, 185701 (2017).
- [84] M. Tarnowski, F. N. Ünal, N. Fläschner, B. S. Rem, A. Eckardt, K. Sengstock, and C. Weitenberg, *Nature Communications* **10**, 1728 (2019).
- [85] M. Heyl, *Reports on Progress in Physics* **81**, 054001 (2018).
- [86] M. Heyl, A. Polkovnikov, and S. Kehrein, *Physical review letters* **110**, 135704 (2013).
- [87] M. Heyl, *Physical review letters* **113**, 205701 (2014).
- [88] E. Torres-Herrera and L. F. Santos, *Physical Review B* **92**, 014208 (2015).

- [89] M. Haque, *Physical Review A* **82**, 012108 (2010).
- [90] J. Mossel and J.-S. Caux, *New Journal of Physics* **12**, 055028 (2010).
- [91] G. Misguich, K. Mallick, and P. Krapivsky, *Physical Review B* **96**, 195151 (2017).
- [92] G. Misguich, N. Pavloff, and V. Pasquier, *SciPost Phys.* **7**, 025 (2019).
- [93] J.-M. Stéphan, *Journal of Statistical Mechanics: Theory and Experiment* **2017**, 103108 (2017).
- [94] L. F. Santos and E. J. Torres-Herrera, in *Chaotic, Fractional, and Complex Dynamics: New Insights and Perspectives* (Springer, 2018) pp. 231–260.
- [95] M. Serbyn and J. E. Moore, *Physical Review B* **93**, 041424 (2016).
- [96] L. F. Santos, F. Borgonovi, and F. Izrailev, *Physical Review Letters* **108**, 094102 (2012).
- [97] L. Santos, *Journal of Physics A: Mathematical and General* **37**, 4723 (2004).
- [98] L. F. Santos and M. Rigol, *Physical Review E* **82**, 031130 (2010).
- [99] L. F. Santos and M. Rigol, *Physical Review E* **81**, 036206 (2010).
- [100] T. A. Brody, J. Flores, J. B. French, P. Mello, A. Pandey, and S. S. Wong, *Reviews of Modern Physics* **53**, 385 (1981).
- [101] V. Oganesyan and D. A. Huse, *Physical Review B* **75**, 155111 (2007).
- [102] Y. Atas, E. Bogomolny, O. Giraud, and G. Roux, *Physical Review Letters* **110**, 084101 (2013).
- [103] M. Garcia-March, S. van Frank, M. Bonneau, J. Schmiedmayer, M. Lewenstein, and L. F. Santos, *New Journal of Physics* **20**, 113039 (2018).
- [104] E. J. Torres-Herrera and L. F. Santos, *Physical Review E* **88**, 042121 (2013).
- [105] D. A. Huse, R. Nandkishore, and V. Oganesyan, *Physical Review B* **90**, 174202 (2014).
- [106] M. Serbyn, Z. Papić, and D. A. Abanin, *Physical Review Letters* **110**, 260601 (2013).
- [107] J. H. Bardarson, F. Pollmann, and J. E. Moore, *Physical Review Letters* **109**, 017202 (2012).
- [108] T. Zhang and G.-B. Jo, *Scientific Reports* **5**, 16044 (2015).
- [109] H. Labuhn, D. Barredo, S. Ravets, S. De Léséleuc, T. Macrì, T. Lahaye, and A. Browaeys, *Nature* **534**, 667 (2016).
- [110] V. Borish, O. Marković, J. A. Hines, S. V. Rajagopal, and M. Schleier-Smith, *Physical Review Letters* **124**, 063601 (2020).
- [111] P. Schauss, *Quantum Science and Technology* **3**, 023001 (2018).
- [112] A. Keesling, A. Omran, H. Levine, H. Bernien, H. Pichler, S. Choi, R. Samajdar, S. Schwartz, P. Silvi, S. Sachdev, P. Zoller, M. Endres, M. Greiner, V. Vuletić, and M. D. Lukin, *Nature* **568**, 207 (2019).
- [113] A. Doçaj, M. L. Wall, R. Mukherjee, and K. R. A. Hazzard, *Physical Review Letters* **116**, 135301 (2016).
- [114] M. L. Wall, N. P. Mehta, R. Mukherjee, S. S. Alam, and K. R. A. Hazzard, *Physical Review A* **95**, 043635 (2017).
- [115] K. R. A. Hazzard, B. Gadway, M. Foss-Feig, B. Yan, S. A. Moses, J. P. Covey, N. Y. Yao, M. D. Lukin, J. Ye, D. S. Jin, and A. M. Rey, *Physical Review Letters* **113**, 195302 (2014).
- [116] L. Reichsöllner, A. Schindewolf, T. Takekoshi, R. Grimm, and H.-C. Nägerl, *Physical Review Letters* **118**, 073201 (2017).
- [117] C.-L. Hung, A. González-Tudela, J. I. Cirac, and H. Kimble, *Proceedings of the National Academy of Sciences* **113**, E4946 (2016).
- [118] C.-Y. Deng, Xiu-Hao Lai and C.-C. Chien, *Physical Review B* **93**, 054116 (2016).
- [119] C. S. Wang, J. C. Curtis, B. J. Lester, Y. Zhang, Y. Y. Gao, J. Freeze, V. S. Batista, P. H. Vaccaro, I. L. Chuang, L. Frunzio, L. Jiang, S. M. Girvin, and R. J. Schoelkopf, *Physical Review X* **10**, 021060 (2020).
- [120] Y. Yanay, J. Braumüller, S. Gustavsson, W. D. Oliver, and C. Tahan, *npj Quantum Information* **6**, 1 (2020).
- [121] I. Arrazola, J. S. Pedernales, L. Lamata, and E. Solano, *Scientific Reports* **6**, 30534 (2016).
- [122] F. Rajabi, S. Motlakunta, C.-Y. Shih, N. Kotibhaskar, Q. Quraishi, A. Ajoy, and R. Islam, *npj Quantum Information* **5**, 1 (2019).
- [123] B. Chiaro, C. Neill, A. Bohrdt, M. Filippone, F. Arute, K. Arya, R. Babbush, D. Bacon, J. Bardin, R. Barends, S. Boixo, D. Buell, B. Burkett, Y. Chen, Z. Chen, R. Collins, A. Dunsworth, E. Farhi, A. Fowler, B. Foxen, C. Gidney, M. Giustina, M. Harrigan, T. Huang, S. Isakov, E. Jeffrey, Z. Jiang, D. Kafri, K. Kechedzhi, J. Kelly, P. Klimov, A. Kourtikov, F. Kostritsa, D. Landhuis, E. Lucero, J. McClean, X. Mi, A. Megrant, M. Mohseni, J. Mutus, M. McEwen, O. Naaman, M. Neeley, M. Niu, A. Petukhov, C. Quintana, N. Rubin, D. Sank, K. Satzinger, A. Vainsencher, T. White, Z. Yao, P. Yeh, A. Zalcman, V. Smelyanskiy, H. Neven, S. Gopalakrishnan, D. Abanin, M. Knap, J. Martinis, and P. Roushan, arXiv:1910.06024 [cond-mat.dis-nn] (2019).
- [124] N. Y. Halpern, C. D. White, S. Gopalakrishnan, and G. Refael, *Physical Review B* **99**, 024203 (2019).
- [125] C. Danieli, A. Andreanov, and S. Flach, *Physical Review B* **102**, 041116(R) (2020).
- [126] P. A. McClarty, M. Haque, A. Sen, and J. Richter, arXiv:2007.01311 (2020).